



UDC 621.371.333:537.874.6

PACS 42.25.Fx

DOI: 10.22363/2658-4670-2022-30-3-231-243

Application of the method of continued boundary conditions to the solution of the problems of wave diffraction on various types of scatterers with complex structure

Dmitry V. Krysanov

*Moscow Technical University of Communications and Informatics,
8a, Aviamotornaya St., Moscow, 111024, Russian Federation*

(received: July 14, 2022; revised: July 18, 2022; accepted: August 8, 2022)

Abstract. The article considers the application of the method of continued boundary conditions to the two-dimensional problem of diffraction of electromagnetic waves by a dielectric body with a cross section of complex geometry and to the problem of diffraction by a Janus sphere in the form of a permeable sphere partially covered by an absolutely soft or an absolutely rigid spherical screen. The results of calculating the scattering pattern for a large set of bodies of different geometry, including fractal-like scatterers, are obtained. It is illustrated that in the case of a smooth body boundary, the algorithm based on the Fredholm equations of the 1st kind makes it possible to obtain results with greater accuracy than for equations of the 2nd kind. The correctness of the method was confirmed by verifying the implementation of the optical theorem for various bodies and by comparing with the results of calculations obtained by other methods.

Key words and phrases: the method of continued boundary conditions, diffraction of waves on bodies of complex geometry, Janus sphere

1. Introduction

In the modern theory of diffraction, there is a growing need for the effective solution of increasingly complex problems, the construction of adequate mathematical models for a wide range of phenomena and processes. This, in turn, requires the development of increasingly universal methods for solving diffraction problems.

In this paper, the method of continued boundary conditions (MCBC) [1] is considered. In MCBC, the surface on which the observation point is chosen, denoted by S_δ , is located outside the scatterer at some sufficiently small distance δ from its boundary S , which is the carrier of the (auxiliary) current and over which integration is carried out. Due to the analyticity of the

© Krysanov D. V., 2022



This work is licensed under a Creative Commons Attribution 4.0 International License

<https://creativecommons.org/licenses/by-nc/4.0/legalcode>

wave field, the boundary condition will be approximately satisfied on the surface S_δ , and as a result, the diffraction problem is solved in an approximate formulation.

The advantages of MCBC are its versatility and simplicity. Moreover, the universality of the MCBC manifests itself, firstly, in the absence of restrictions on the geometry of the scatterer (including it is applicable both for scatterers with border breaks and for thin screens), and secondly, in the possibility of reducing the boundary value problem to Fredholm integral equations of the 1st, and of the 2nd kind [2]. In addition, when solving problems of diffraction on thin screens with the help of MCBC, it is easy to reduce the original boundary value problem to integral equations, both in the case of E- and in the case of H-polarization of the incident field (or problems of diffraction by bodies, on the boundary of which both the Dirichlet conditions and the Neumann conditions are satisfied). This is much more difficult to do, for example, when using the method of current integral equations. Another advantage of the MCBC is the ability to use various basis functions when solving the corresponding integral equations.

However, MCBC is an approximate approach, and computational algorithms based on MCBC have a lower convergence rate than, for example, algorithms based on discrete source method (in cases where the latter is applicable). At the same time, it is possible to improve the accuracy when using various basic functions (for example, splines) within the framework of the MCBC.

As an example of the application of MCBC, the problem of wave diffraction by a dielectric body of complex geometry is considered, which is very relevant and remains relatively poorly studied due to the complexity of its solution. The results of modeling the characteristics of wave scattering by dielectric bodies are of great interest in such areas as, for example, the optics of inhomogeneous media, laser flaw detection, the design of absorbing coatings, etc. [3].

The problem of diffraction on the Janus sphere in the form of a penetrable sphere partially covered by an absolutely soft or absolutely rigid spherical screen is also considered. Janus particles are of great interest in antenna engineering, medicine, and biology [4, 5]. Despite the practical significance of Janus particles, the scattering of waves by such structures has been studied rather poorly. There are a number of works in the literature devoted to both acoustic and electromagnetic problems of diffraction on the Janus sphere [6–9].

2. Solution of the problem of wave diffraction by a dielectric body of complex geometry

Let primary electromagnetic field $\mathbf{E}^0, \mathbf{H}^0$, be incident on an infinitely long magnetodielectric cylinder with a generator parallel to axis Oz and guide S . The geometry of the problem is shown in figure 1. Consider the case of E-polarization, when electric field intensity vector \mathbf{E} has only one component E_z (below denoted by the letter U_- or U_+) parallel to the cylindrical body generator. The following coupling conditions will then take place at the boundary of the scatterer:

$$U_+|_S = U_-|_S, \quad \frac{\partial U_+}{\partial n} \Big|_S = \kappa \frac{\partial U_-}{\partial n} \Big|_S, \tag{1}$$

where U_+ is the field inside the cylinder; $U_- = U^0 + U^1$ is the full field outside the body, where U^0 is falling and U^1 is scattered (secondary) fields; $\partial/\partial n$ is differentiation in the direction of the normal internal to S ; and $\kappa = \mu_i/\mu_e$, where μ_i and μ_e are the relative magnetic permeabilities of the media inside and outside the body, respectively. The external medium ($D_e = \mathbb{R}^2 \setminus \bar{D}$, $\bar{D} = D \cup S$, where D is the area bounded by curve S) and the medium inside the cylinder are assumed to be homogeneous, linear, and isotropic. At infinity, the standard radiation conditions for the scattered field are assumed to be met.

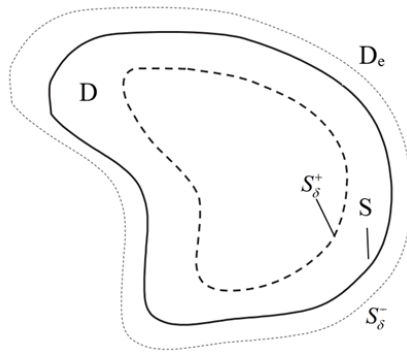


Figure 1. The geometry of the diffraction problem

Let us use the following representations to solve the Helmholtz equation in regions D and D_e , respectively [10]:

$$\begin{aligned}
 U_-(\mathbf{r}) &= U^0(\mathbf{r}) + \int_S \left\{ \frac{\partial U_-(\mathbf{r}')}{\partial n'} G_-(\mathbf{r}; \mathbf{r}') - U_-(\mathbf{r}') \frac{\partial G_-(\mathbf{r}; \mathbf{r}')}{\partial n'} \right\} ds', \\
 U_+(\mathbf{r}) &= - \int_S \left\{ \frac{\partial U_+(\mathbf{r}')}{\partial n'} G_+(\mathbf{r}; \mathbf{r}') - U_+(\mathbf{r}') \frac{\partial G_+(\mathbf{r}; \mathbf{r}')}{\partial n'} \right\} ds',
 \end{aligned} \tag{2}$$

in which $G_{\pm}(\mathbf{r}; \mathbf{r}') = \frac{1}{4i} H_0^{(2)}(k_{\pm}|\mathbf{r} - \mathbf{r}'|)$ are the fundamental solutions of the scalar Helmholtz equation in \mathbb{R}^2 with material parameters of the media D_e and D , respectively, k_+ and k_- are the wavenumbers of the medium inside and outside the scatterer. Demanding, in accordance with MCBC, the fulfillment of conditions Eqs. (1) to be met on contour S_{δ}^- located in $\mathbb{R}^2 \setminus \bar{D}$, and on contour S_{δ}^+ located in area D (see figure 1) using equations (2), we obtain the following systems of the Fredholm integral equations of the first or second kind, respectively:

$$\begin{aligned}
& \int_S \left\{ \frac{\partial U(\mathbf{r}')}{\partial n'} (G_-(\mathbf{r}_-; \mathbf{r}') + \kappa G_+(\mathbf{r}_+; \mathbf{r}')) - \right. \\
& \quad \left. - U(\mathbf{r}') \left(\frac{\partial G_-(\mathbf{r}_-; \mathbf{r}')}{\partial n'} + \frac{\partial G_+(\mathbf{r}_+; \mathbf{r}')}{\partial n'} \right) \right\} ds' = -U^0(\mathbf{r}_-), \\
& \int_S \left\{ \frac{\partial U(\mathbf{r}')}{\partial n'} \left(\frac{\partial G_-(\mathbf{r}_-; \mathbf{r}')}{\partial n} + \frac{\partial G_+(\mathbf{r}_+; \mathbf{r}')}{\partial n} \right) - \right. \\
& \quad \left. - U(\mathbf{r}') \left(\frac{\partial^2 G_-(\mathbf{r}_-; \mathbf{r}')}{\partial n \partial n'} + \frac{1}{\kappa} \frac{\partial^2 G_+(\mathbf{r}_+; \mathbf{r}')}{\partial n \partial n'} \right) \right\} ds' = -\frac{\partial U^0(\mathbf{r}_-)}{\partial n},
\end{aligned} \tag{3}$$

$$\begin{aligned}
U(\mathbf{r}) &= \frac{1}{2} U^0(\mathbf{r}_-) + \frac{1}{2} \int_S \left\{ \frac{\partial U(\mathbf{r}')}{\partial n'} (G_-(\mathbf{r}_-; \mathbf{r}') - \kappa G_+(\mathbf{r}_+; \mathbf{r}')) - \right. \\
& \quad \left. - U(\mathbf{r}') \left(\frac{\partial G_-(\mathbf{r}_-; \mathbf{r}')}{\partial n'} - \frac{\partial G_+(\mathbf{r}_+; \mathbf{r}')}{\partial n'} \right) \right\} ds', \\
\frac{\partial U(\mathbf{r})}{\partial n} &= \frac{1}{1+\kappa} \frac{\partial U^0(\mathbf{r}_-)}{\partial n} + \frac{1}{1+\kappa} \int_S \left\{ \frac{\partial U(\mathbf{r}')}{\partial n'} \left(\frac{\partial G_-(\mathbf{r}_-; \mathbf{r}')}{\partial n} - \right. \right. \\
& \quad \left. \left. - \kappa \frac{\partial G_+(\mathbf{r}_+; \mathbf{r}')}{\partial n} \right) - U(\mathbf{r}') \left(\frac{\partial^2 G_-(\mathbf{r}_-; \mathbf{r}')}{\partial n \partial n'} - \frac{\partial^2 G_+(\mathbf{r}_+; \mathbf{r}')}{\partial n \partial n'} \right) \right\} ds',
\end{aligned} \tag{4}$$

where observation points $M(\mathbf{r}_\pm)$ belong to contours S_δ^\pm and point $M(\mathbf{r}) \in S$ and it is denoted that $U = U_-$. Note that the contours that are separated from S by a fairly small distance δ are most often chosen as S_δ^\pm ; i.e., equidistant contours are considered [1, 10]. Further, to solve system of equations (3), (4), the Krylov–Bogolyubov method is used. A generalization of the method to the problem of diffraction by a cylindrical body located in a homogeneous magnetodielectric half-space is given in [11].

Let us consider the results of numerical modeling. Thereafter, we will assume that the body is irradiated by a plane wave. As an example, let us first consider the diffraction problem on an elliptical cylinder, a cylinder with a quadrifolium cross section, and a cylinder with a rectangular cross-section. Figure 2 shows the angular dependences of the scattering pattern for the corresponding geometry obtained for the following values of the problem parameters: $k\delta = 10^{-4}$, $\varphi_0 = 0$, $\mu_i = 1$, $\varepsilon_i = 4$ (the material parameters of the external medium are $\mu_e = 1$, $\varepsilon_e = 1$ everywhere). The dimensions of the bodies had the following values: the semiaxis or half the side lengths of the rectangle $ka = 5$, $kb = 1$ and the $ka = 5$, $\tau = 0.5$ parameters for the body with a cross section in the form of a quadrifolium. The results were compared with the patterns constructed using the modified discrete source method [10, 12]. Note that the modified discrete source method cannot be directly applied to the problem of the diffraction on bodies that have boundary breaks, and so the contour of the axial section of the body was approximated by a smooth contour to solve the problem using the modified discrete source method [12].

Note also that the modified discrete source method provides high accuracy of calculation for bodies with a smooth border, such as ellipses, multifoil, etc.

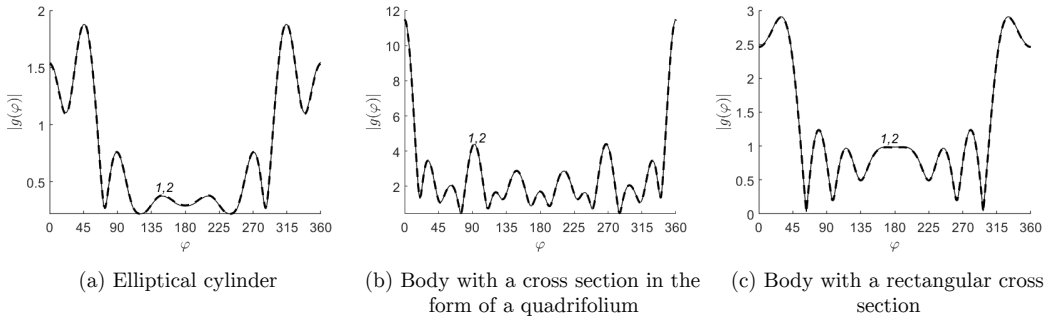


Figure 2. The angular dependence of the scattering pattern for different bodies: (1) the modified discrete source method and (2) the continued boundary conditions method

Figures 3 and 4 illustrate the angular dependences of the scattering pattern for the fractal-like cylinders with a cross section in the form of a Koch snowflake and Sierpinski curve (first iteration) [13] at the problem parameters of $k\delta = 10^{-4}$, $\mu_i = 1$, $\varepsilon_i = 4$. The maximum cross-sectional size of a body with a cross section in the form of the Koch snowflake and a body with a cross section in the form of the Sierpinski curve on the x axis was $kL = 10$. Two different angles of incidence $\varphi_0 = 0$ and $\varphi_0 = 45^\circ$ were considered. As follows from the figures for the geometry under study, the maximum points of the angular dependences of the scattering pattern roughly coincide with the angles of incidence of the plane wave. It can also be seen that the dependences of the pattern for both a body with a section in the form of the Koch snowflake and a body with a section in the form of the Sierpinski curve have quite large side lobes.

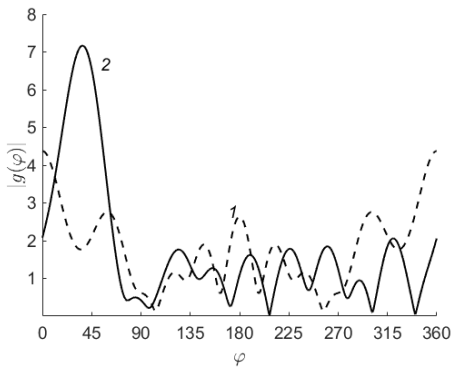


Figure 3. The angular dependence of the scattering pattern for a body with a cross section in the form of a Koch snowflake. The angle of incidence of the wave (1) $\varphi_0 = 0$ and (2) $\varphi_0 = 45^\circ$

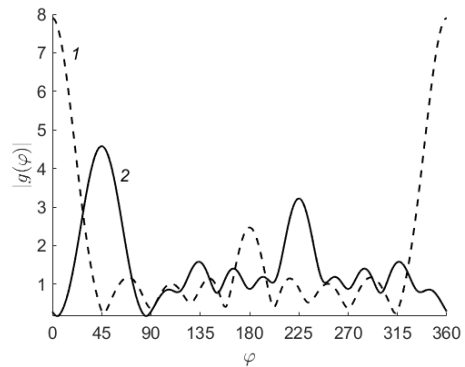


Figure 4. The angular dependence of the scattering pattern for a body with a cross section in the form of a Sierpinski curve. The angle of incidence of the wave (1) $\varphi_0 = 0$ and (2) $\varphi_0 = 45^\circ$

Table 1 shows the differences in the scattering pattern modules of the specified geometry obtained by two methods: using the modified discrete source method and the continued boundary conditions method. As can be seen from the table 1, the difference in results decreases as the number of basic functions used increases. It also follows from the given data that for bodies with a smooth boundary, the use of the Fredholm equations of the 1st kind is more preferable, due to faster convergence. In the case of a body with a rectangular section, the use of Fredholm equations of the 2nd kind gives better results.

Table 1

Comparison of the results obtained using the modified discrete source method and the continued boundary conditions method

N	System of integral equations of the first kind		System of integral equations of the second kind	
	absolute error	relative error	absolute error	relative error
Diffraction on an elliptical cylinder				
48	$1.295 \cdot 10^{-2}$	2.038%	$1.453 \cdot 10^{-1}$	24.297%
96	$1.904 \cdot 10^{-3}$	0.230%	$4.183 \cdot 10^{-2}$	7.238%
192	$6.096 \cdot 10^{-4}$	0.067%	$1.144 \cdot 10^{-2}$	2.003%
288	$5.834 \cdot 10^{-4}$	0.075%	$5.539 \cdot 10^{-3}$	0.977%
384	$5.607 \cdot 10^{-4}$	0.075%	$3.450 \cdot 10^{-3}$	0.612%
Diffraction on a body with a cross section in the form of a quadrifolium				
48	$1.643 \cdot 10^{-1}$	10.411%	$3.836 \cdot 10^{-1}$	21.169%
96	$2.499 \cdot 10^{-2}$	1.442%	$9.462 \cdot 10^{-2}$	5.125%
192	$5.802 \cdot 10^{-3}$	0.325%	$2.534 \cdot 10^{-2}$	1.370%
288	$2.984 \cdot 10^{-3}$	0.166%	$1.143 \cdot 10^{-2}$	0.619%
384	$2.176 \cdot 10^{-3}$	0.121%	$6.474 \cdot 10^{-3}$	0.351%
Diffraction on a body with a rectangular cross section				
48	$3.498 \cdot 10^{-2}$	4.781%	$5.035 \cdot 10^{-2}$	6.795%
96	$1.466 \cdot 10^{-2}$	1.956%	$1.417 \cdot 10^{-2}$	1.715%
192	$7.358 \cdot 10^{-3}$	0.879%	$4.773 \cdot 10^{-3}$	0.466%
288	$5.229 \cdot 10^{-3}$	0.561%	$3.122 \cdot 10^{-3}$	0.248%
384	$4.219 \cdot 10^{-3}$	0.429%	$2.641 \cdot 10^{-3}$	0.208%

3. Solution to the problem of wave diffraction on the Janus sphere

Let us consider the mathematical formulation of the problem. Let a homogenous sphere of radius a be covered with an infinitely thin spherical screen S with an opening angle $2\theta_J$. We introduce a spherical coordinate system in which the z is directed along the axis of the considered body of revolution (the Janus sphere). The geometry of the problem is depicted in figure 5.

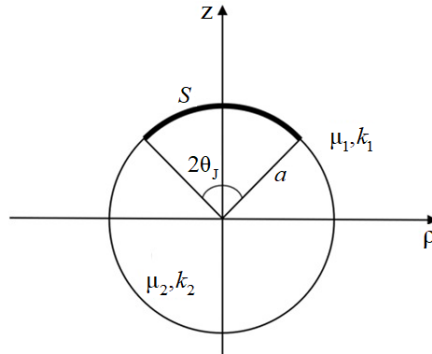


Figure 5. Axial section of a Janus sphere

We suppose that the wavenumbers and medium densities outside and inside the sphere are equal to k_1, μ_1 and k_2, μ_2 , respectively. Thus, the wave field outside and inside the sphere satisfies the homogeneous Helmholtz equations

$$\begin{aligned} \Delta U + k_1^2 U &= 0, & r > a, \\ \Delta U + k_2^2 U &= 0, & 0 < r < a, \end{aligned} \quad (5)$$

where r is the radial coordinate in the spherical coordinate system. For the sake of brevity, we consider only the case of an absolutely soft spherical screen. Then the boundary conditions on the surface of the screen have the form

$$U|_{r=a, \theta < \theta_J} = 0. \quad (6)$$

At $\theta \in (\theta_J, \pi)$, the matching conditions are satisfied:

$$[U] = 0, \quad \left[\frac{1}{\mu} \frac{\partial U}{\partial r} \right] = 0, \quad (7)$$

where μ is the density ($\mu = \mu_1$ for $r > a$, $\mu = \mu_2$ for $r < a$) and the square brackets indicate a jump of the corresponding quantity. We assume that the Janus sphere is irradiated by a plane wave, which has the form

$$U_{\text{inc}} = \exp(-ik_1 r (\sin \theta \sin \theta_0 \cos \varphi + \cos \theta \cos \theta_0)). \quad (8)$$

Here, θ_0 is the angle of incidence of the plane wave. The scattered field U^1 satisfies the radiation condition at infinity. The total field also satisfies the Meixner condition at the edge of the spherical screen.

Let us apply the MCBC for solving the posed diffraction problem. For this purpose, we represent the field outside the permeable sphere in the form

$$U(\mathbf{r}) = U^0(\mathbf{r}) - \int_S J(\mathbf{r}')G(\mathbf{r}, \mathbf{r}')ds'. \tag{9}$$

Here, $U^0(\mathbf{r})$ is the primary field determined from the solution of the diffraction problem on the sphere in the absence of the screen,

$$J(\mathbf{r}') \equiv J(\theta', \varphi') = \left[\frac{\partial U}{\partial r'} \right]_{\substack{r=a \\ \theta < \theta_J}}.$$

In equations (9) $G(\mathbf{r}, \mathbf{r}')$ is the Green function of the permeable sphere; for $r > a$, it has the form

$$G = G_0 + G_1, \tag{10}$$

where

$$G_0 = \frac{e^{-ik_1R}}{4\pi R}, \quad R = |\mathbf{r} - \mathbf{r}'|, \tag{11}$$

$$G_1 = \frac{k_1}{4\pi i} \sum_{n=0}^{\infty} (2n + 1)V_n H_n^{(2)}(k_1 r') H_n^{(2)}(k_1 r) P_n(\cos \gamma), \tag{12}$$

$$\cos \gamma = \sin \theta \sin \theta' \cos(\varphi - \varphi') + \cos \theta \cos \theta', \tag{13}$$

$$V_n = \frac{\mu_{12} J_n(k_1 a) \eta_n(k_2 a) - \eta_n(k_1 a) J_n(k_2 a)}{\xi_n(k_1 a) J_n(k_2 a) - \mu_{12} H_n^{(2)}(k_1 a) \eta_n(k_2 a)}, \tag{14}$$

$$\mu_{12} = \frac{\mu_1}{\mu_2}, \quad \eta_n(x) = x J'_n(x), \quad \xi_n(x) = x H_n^{(2)'}(x), \tag{15}$$

and $J_n(x)$, $H_n^{(2)}(x)$ are the spherical Bessel and Hankel functions, respectively, $P_n(x)$ — Legendre polynomials. Note that the primary field outside the sphere has the form

$$U^0(\mathbf{r}) = U_{\text{inc}}(\mathbf{r}) + \sum_{n=-\infty}^{\infty} i^{-n} (2n + 1) V_n H_n^{(2)}(k_1 r) P_n(\cos \gamma_0), \tag{16}$$

where $\cos \gamma_0(\theta, \varphi) = \sin \theta \sin \theta_0 \cos \varphi + \cos \theta \cos \theta_0$.

According to the standard scheme of the MCBC, we then substitute formula (9) into boundary condition (6) imposed on the auxiliary surface S_δ shifted by a small distance δ from the surface S [1, 10, 14]. As a result, the problem will be reduced to solving a two-dimensional Fredholm integral equation of the first kind, which has the following form in spherical coordinates:

$$\int_0^{2\pi} \int_0^{\theta_J} K(\theta, \varphi, \theta', \varphi') J(\theta', \varphi') \sin \theta' d\theta' d\varphi' = B(\theta, \varphi), \tag{17}$$

$$\theta \in [0, \theta_J], \quad \varphi \in [0, 2\pi],$$

where $K(\theta, \varphi, \theta', \varphi') = a^2 G|_{r'=a, r=a+\delta}$, $B(\theta, \varphi) = U^0|_{r=a+\delta}$.

Equation (17) was solved using a piecewise-constant approximation of an unknown function with subsequent application of the Krylov–Bogolyubov method. The kernel of Eq. (17) was found using the acceleration of the convergence of series (12). In order to speed up the convergence of this series, the asymptotic behavior of the n -th term of the series as $n \rightarrow \infty$ was distinguished (this quantity can be called the singular part of the Green's function). The singular part of the Green's function was summarized analytically using the generating function of the Legendre polynomials. The remaining (regular) part of the Green's function was a fairly fast convergent series. A detailed derivation of the main relations, as well as the case of an absolutely rigid screen, was considered in [15].

Let us consider results of the numerical simulation. The results of calculating the intensity of the scattered field in the far zone for the Janus sphere were compared with the results obtained using the T-matrix method, which are given in [9]. The acoustic problem of diffraction was considered [9]. The wavenumbers and densities of the media inside and outside the sphere were equal to $k_1 = 1$, $\mu_1 = 1$ and $k_2 = 1.5$, $\mu_2 = 1.5$, respectively. Parameter δ in using the MCBC was taken to be 10^{-3} in all cases. The angle of incidence of the primary wave $\theta_0 = 0^\circ$. Sphere radius $k_1 a = 6$. The half-opening angle was equal to $\theta_J = 90^\circ$. The number of collocation points along both angular coordinates $N_1 = 25$, $N_2 = 100$. Figure 6 shows the angular dependences of the scattered field intensity obtained using the T-matrix method (curve 1) and using the proposed approach based on the MCBC (curve 2). It can be seen from Fig. 6 that the results coincide with graphic accuracy in the case of the Dirichlet condition. Due to the presence of the second normal derivative of the Green's function in the case of the Neumann condition on the screen, the accuracy of calculating the diagram using the MCBC is somewhat lower than in the case of the Dirichlet condition. For the considered problem, the accuracy of the optical theorem was verified. Calculations showed that the relative error in the fulfillment of the optical theorem did not exceed 2%.

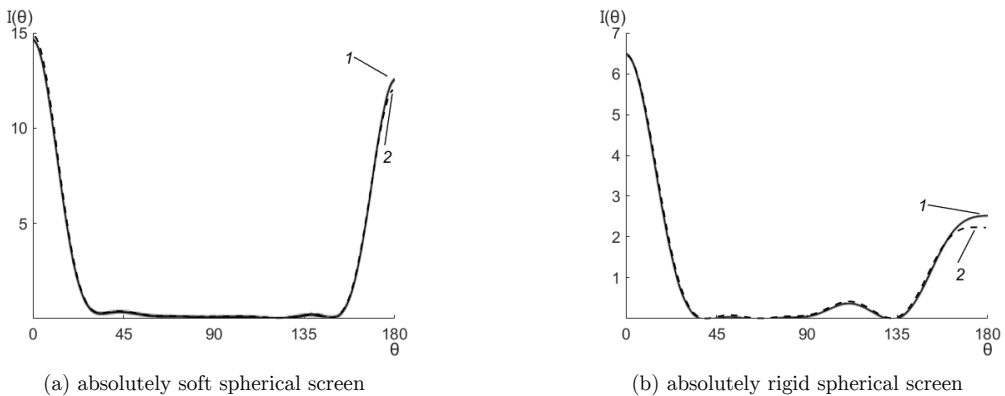


Figure 6. Angular dependences of the intensity of the scattered field of a Janus sphere in the form of a penetrable sphere partially covered with spherical screen, obtained using the T-matrix method and using an algorithm based on MCBC

Figure 7 depicts angular dependences of the scattered field intensity on the opening angle of the spherical screen. Curve 1 corresponds to diffraction by a permeable sphere not covered by a screen. Curve 6 in the figures shows the dependences obtained for the intensity upon diffraction of a plane wave by an absolutely soft (Fig. 7a) or absolutely rigid (Fig. 7b) sphere of the corresponding wave size using the modified discrete source method (MDSM) [16]. Curves 2–5 correspond to screen half-opening angles equal to 45° , 90° , 135° , and 179° . The wave size of the Janus sphere and the angle of incidence of the wave are $k_1 a = 6$, $\theta_0 = 0$. The material parameters of the media and wavenumbers are the same as for previous figure. It can be seen from the figure that in the case when the screen almost completely covers the sphere (curve 5), the scattered field intensity graph coincides with the results for a perfectly reflecting sphere, which corresponds to the physical picture of the phenomenon under consideration. It is also seen that in all cases there is a sharp intensity maximum in the direction of the angle of incidence of the plane wave. In the case of a soft screen, the magnitude of the maximum has the greatest value for $\theta_J = 179^\circ$ (that is, when the screen degenerates into a sphere). In the absence of a screen (that is, in the case of diffraction by a permeable sphere), the maximum in the direction of wave incidence is even greater (than for a covered sphere). In the backscattering direction (at $\theta = 180^\circ$), there is also an intensity maximum, which takes on the largest values at $\theta_J = 45^\circ$ and $\theta_J = 90^\circ$. In the case of an absolutely rigid screen, the value of the intensity maximum in the direction of incidence of a plane wave is much greater for $\theta_J = 45^\circ$ compared to other screen opening angles. The backscatter level is also maximum at $\theta_J = 45^\circ$.

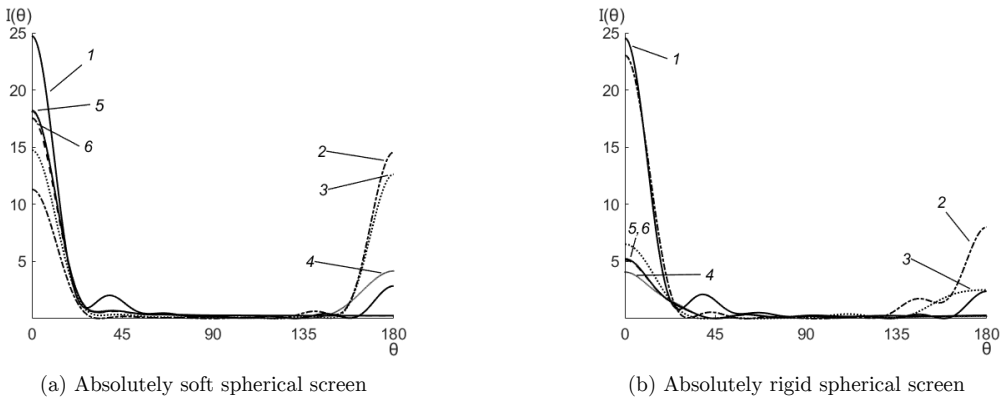


Figure 7. Angular dependences of the intensity of the scattered field of the Janus sphere for different opening angles of a spherical screen covering it

4. Conclusions

Based on the method of continued boundary conditions, an algorithm for solving the two-dimensional problem of plane wave diffraction by dielectric bodies with complex cross-sectional geometry is shown. A comparison is made with the results obtained using modified discrete source method. It is shown

that the MCBC makes it possible to obtain the results of scattering diagram calculations with a sufficiently high accuracy. The results of calculating the scattering diagram for a large set of bodies of different geometry, including fractal-like scatterers, are obtained. It is illustrated that in the case of a smooth body boundary, the algorithm based on the Fredholm equations of the 1st kind allows obtaining results with greater accuracy than for equations of the 2nd kind.

An algorithm for solving the scalar diffraction problem on the Janus sphere is shown on the basis of the MCBC. The results of calculating the intensity of the scattered field obtained using the proposed method are compared with the results found using the T-matrix method. It has been shown that the results coincide well. The angular dependences of the intensity of the scattered field for various opening angles of the reflecting screen are constructed and studied. A significant difference is shown between the behavior of the angular dependences of the intensity in the case of an absolutely soft and absolutely rigid screen.

References

- [1] A. G. Kyurkchan and A. P. Anyutin, "The method of continued boundary conditions and wavelets," *Doklady Mathematics*, vol. 66, no. 1, pp. 132–135, 2002.
- [2] A. G. Kyurkchan and A. P. Anyutin, "The well-posedness of the formulation of diffraction problems reduced to Fredholm integral equations of the first kind with a smooth kernel," *Journal of Communications Technology and Electronics*, vol. 51, no. 7, pp. 48–51, 2006. DOI: 10.1134/S1064226906010062.
- [3] M. I. Mishchenko, N. T. Zakharova, N. G. Khlebtsov, G. Videen, and T. Wriedt, "Comprehensive thematic T-matrix reference database: A 2015–2017 update," *Journal of Quantitative Spectroscopy and Radiative Transfer*, vol. 202, pp. 240–246, 2017. DOI: 10.1016/j.jqsrt.2017.08.007.
- [4] J. Zhang, B. A. Grzybowski, and S. Granick, "Janus particle synthesis, assembly, and application," *Langmuir*, vol. 33, no. 28, pp. 6964–6977, 2017. DOI: 10.1021/acs.langmuir.7b01123.
- [5] M. Lattuada and T. A. Hatton, "Synthesis, properties and applications of Janus nanoparticles," *Nano Today*, vol. 6, no. 3, pp. 286–308, 2011. DOI: 10.1016/j.nantod.2011.04.008.
- [6] D. Kim, E. J. Avital, and T. Miloh, "Sound scattering and its reduction by a Janus sphere type," *Advances in Acoustics and Vibration*, vol. 2014, no. 392138, 2014. DOI: 10.1155/2014/392138.
- [7] A. Gillman, "An integral equation technique for scattering problems with mixed boundary conditions," *Advances in Computational Mathematics*, vol. 43, no. 2, pp. 351–364, 2017. DOI: 10.1007/s10444-016-9488-6.
- [8] S. C. Hawkins, T. Rother, and J. Wauer, "A numerical study of acoustic scattering by Janus spheres," *The Journal of the Acoustical Society of America*, vol. 147, no. 6, pp. 4097–4105, 2020. DOI: 10.1121/10.0001472.

- [9] T. Rother, *Sound scattering on spherical objects*. Heidelberg: Springer, 2020.
- [10] A. G. Kyurkchan and N. I. Smirnova, *Mathematical modeling in diffraction theory: based on a priori information on the analytical properties of the solution*. Amsterdam: Elsevier, 2015.
- [11] D. V. Krysanov, A. G. Kyurkchan, and S. A. Manenkov, “Application of the method of continued boundary conditions to the solution of the problem of wave diffraction on scatterers of complex geometry located in homogeneous and heterogeneous media,” *Optics and Spectroscopy*, vol. 128, no. 4, pp. 481–489, 2020. DOI: 10.1134/S0030400X20040141.
- [12] A. G. Kyurkchan and S. A. Manenkov, “Application of different orthogonal coordinates using modified method of discrete sources for solving a problem of wave diffraction on a body of revolution,” *Journal of Quantitative Spectroscopy and Radiative Transfer*, vol. 113, no. 18, pp. 2368–2378, 2012. DOI: 10.1016/j.jqsrt.2012.05.010.
- [13] R. M. Crownover, *Intoduction to fractals and chaos*. Boston: Jones and Bartlett Publishers, 1995.
- [14] A. G. Kyurkchan and S. A. Manenkov, “Solution of the problem of diffraction by a plane screen in a plane layered medium with the help of the method of continued boundary conditions,” *Journal of Communications Technology and Electronics*, vol. 65, no. 7, pp. 778–786, 2020. DOI: 10.1134/S1064226920060200.
- [15] D. V. Krysanov, A. G. Kyurkchan, and S. A. Manenkov, “Two approaches to solving the problem of diffraction on a Janus sphere,” *Acoustical Physics*, vol. 67, no. 2, pp. 108–119, 2021. DOI: 10.1134/S1063771021020020.
- [16] S. A. Manenkov, “A new version of the modified method of discrete sources in application to the problem of diffraction by a body of revolution,” *Acoustical Physics*, vol. 60, no. 2, pp. 127–133, 2014. DOI: 10.1134/S1063771014010102.

For citation:

D. V. Krysanov, Application of the method of continued boundary conditions to the solution of the problems of wave diffraction on various types of scatterers with complex structure, *Discrete and Continuous Models and Applied Computational Science* 30 (3) (2022) 231–243. DOI: 10.22363/2658-4670-2022-30-3-231-243.

Information about the authors:

Krysanov, Dmitry V. — postgraduate student of Department of Probability Theory and Applied Mathematics of Moscow Technical University of Communications and Informatics (e-mail: d.v.krysanov@mtuci.ru, phone: +7(903)5418711, ORCID: <https://orcid.org/0000-0001-5100-3007>)

УДК 621.371.333:537.874.6

PACS 42.25.Fx

DOI: 10.22363/2658-4670-2022-30-3-231-243

Применение метода продолженных граничных условий к решению задач дифракции на различных типах частиц сложной структуры

Д. В. Крысанов

*Московский технический университет связи и информатики,
ул. Авиамоторная, д. 8а, Москва, 111024, Россия*

Аннотация. В статье рассмотрено применение метода продолженных граничных условий к двумерной задаче дифракции электромагнитных волн на диэлектрическом теле с поперечным сечением сложной геометрии и к задаче дифракции на сфере Януса в виде пронизываемого шара, частично покрытого абсолютно мягким или абсолютно жёстким сферическим экраном. Получены результаты расчёта диаграммы рассеяния для большого набора тел разной геометрии, в том числе фракталоподобных рассеивателей. Проиллюстрировано, что в случае гладкой границы тела алгоритм на основе уравнений Фредгольма 1-го рода позволяет получать результаты с большей точностью, чем для уравнений 2-го рода. Корректность метода подтверждена при помощи проверки выполнения оптической теоремы для различных тел и путём сравнения с результатами расчётов, полученных другими методами.

Ключевые слова: метод продолженных граничных условий, дифракция волн на телах сложной геометрии, сфера Януса